

RESEARCH

Open Access

Identification of a Histidine Metal Ligand in the *argE*-Encoded *N*-Acetyl-L-Ornithine Deacetylase from *Escherichia coli*

Wade C McGregor⁴, Danuta M Gillner^{2,3}, Sabina I Swierczek¹, Dali Liu^{2*} and Richard C Holz^{1,2*}

Abstract

The H355A, H355K, H80A, and H80K mutant enzymes of the *argE*-encoded *N*-acetyl-L-ornithine deacetylase (ArgE) from *Escherichia coli* were prepared, however, only the H355A enzyme was found to be soluble. Kinetic analysis of the Co(II)-loaded H355A exhibited activity levels that were 380-fold less than Co(II)-loaded WT ArgE. Electronic absorption spectra of Co(II)-loaded H355A-ArgE indicate that the bound Co(II) ion resides in a distorted, five-coordinate environment and Isothermal Titration Calorimetry (ITC) data for Zn(II) binding to the H355A enzyme provided a dissociation constant (K_d) of 39 μ M. A three-dimensional homology model of ArgE was generated using the X-ray crystal structure of the *dapE*-encoded *N*-succinyl-L,L-diaminopimelic acid desuccinylase (DapE) from *Haemophilus influenzae* confirming the assignment of H355 as well as H80 as active site ligands.

Keywords: Zinc; Bioinorganic Chemistry; Hydrolysis; Deacetylase; Active site ligands; Isothermal titration calorimetry; Mechanistic enzymology

Prokaryotes synthesize arginine through a series of eight enzymatically-catalyzed reactions that differ from those of eukaryotes by two key steps: i) acetylation of glutamate and ii) the subsequent deacetylation of the arginine precursor *N*^α-acetyl-L-ornithine (L-NAO) by the *argE*-encoded *N*^α-acetyl-L-ornithine deacetylase (ArgE) (Figure 1) (Cunin et al. 1986; Davis 1986; Ledwidge and Blanchard 1999). The arginine biosynthetic pathway is found in all Gram-negative and most Gram-positive bacteria including all of the so-called ESKAPE pathogens (*Enterococcus faecium*, *Staphylococcus aureus*, *Klebsiella pneumoniae*, *Acinetobacter baumannii*, *Pseudomonas aeruginosa*, and *Enterobacter* species), which account for more than 60% of the multidrug resistant hospital acquired infections in the United States (Velasco et al. 2002; Cunin et al. 1986; Sakanian et al. 1990; Xu et al. 2000; Sakanyan et al. 1996; Hani et al. 1999; Valentsev et al. 1995; Picard and Dillon 1989). Because ornithine is required, not only for the synthesis of arginine in bacteria, but also for

the production of polyamines involved in DNA replication and cell division, the L-NAO deacetylation step is critical for bacterial proliferation (Girodeau et al. 1986). Indeed, when an arginine auxotrophic bacterial strain void of L-NAO deacetylase activity was transformed with a plasmid containing *argE*, an Arg⁺ phenotype resulted (Meinell et al. 1992). However, when the start codon (ATG) of *argE* in the same plasmid was changed to the Amber codon (TAG), the resultant plasmid was unable to relieve arginine auxotrophy in the same cell strain indicating that ArgE is required for cell viability. Given the fact that ArgE is only found in prokaryotes and is required for bacterial cell growth and proliferation, it represents a potential enzymatic target for the development of a new class of antimicrobial agents (Girodeau et al. 1986).

At the present time, no X-ray crystallographic data is available for any ArgE enzyme but it shares sequence homology with several dinuclear Zn(II) metallopeptidases in the M28 family and biochemical studies revealed that the ArgE from *E. coli* is a Zn(II) containing enzyme (Javid-Majd and Blanchard 2000; McGregor et al. 2005; Holz 2002; Holz et al. 2003). Based on sequence alignments of the ArgE from *E. coli* with the aminopeptidase from *Aeromonas proteolytica* (AAP) (Desmarais et al. 2006), the *dapE*-

* Correspondence: dliuluc@gmail.com; richard.holz@marquette.edu

²Chemistry and Biochemistry, Loyola University Chicago, Chicago, IL 60626, USA

¹Contribution from the Department of Chemistry, Marquette University, Milwaukee, WI 53233, USA

Full list of author information is available at the end of the article

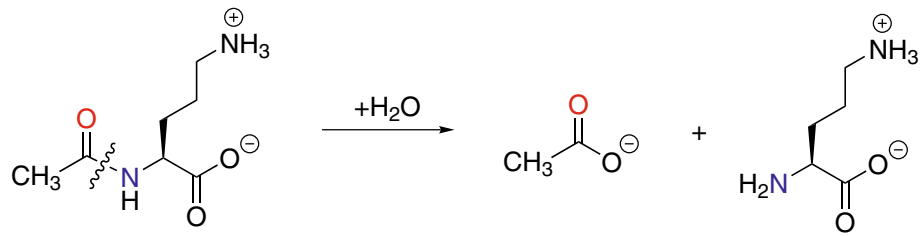


Figure 1 Reaction catalyzed by ArgE.

encoded *N*-succinyl-L,L-diaminopimelic acid desuccinylase (DapE) (Nocek et al. 2010), the *N*-acetyl-L-citrulline deacetylase (ACD) from *Xanthomonas campestris* (Shi et al. 2007), and the carboxypeptidase from *Pseudomonas sp* strain-RS-16 (CPG₂) (Rowell et al. 1997), the residues that function as ligands in the dinuclear active site of AAP, DapE, ACD, and CPG₂ are strictly conserved in ArgE (Figure 2) (Born et al. 1998; Chevrier et al. 1994; Rowell

et al. 1997). Since AAP, DapE, and CPG₂ possess a (μ-aquo)(μ-carboxylato)dizinc(II) core with one terminal carboxylate and one histidine residue at each metal site, a similar active site was proposed for ArgE (Tao et al. 2012).

In an effort to provide insight into the structural properties of each divalent metal ion in the active site of the ArgE from *E. coli*, we have prepared and purified the H355A, H355K, H80A, and H80K ArgE mutant enzymes.

```

ArgE_Ec      -----MKNKLPFFIEIYRALIATPSISATEEALDQSNADLITLLADWFKDLG 47
DapE_Hi     -----MKEKV---VSLAQDLIRRPISLSPNDEGCQQ-----IIAERLEKLG 37
ACD_Xc      -----MTDLLASTLEHLETLVFSFDRNPPRAIAAEGG-----IFDYLRQL 41
CPG2_Ps     ALAQKRDNVLFQAATDEQPAVIKLTLEKLVNIETGTGDAEGIAAAG---NFLEAELKNLG 56
              .: .: .*: .: .: .: .:

ArgE_Ec      FNVEVQVPVPGTRKFNML-ASIGQGAGLLLAGHTDTPVFDD-GRWTRDPFTEHDGKGL 105
DapE_Hi     FQIEWMPFN---DTLNLW-AKHGTSEPVIAFAGHTDVVPTGDNQWSSPPFSAEIIDGML 93
ACD_Xc      PGFQVEVIDHGDGAVSLY-AVRGT--PKYLFNVHLDVVPDSP--HWSADPHVMRRTEDRV 96
CPG2_Ps     FTVTRSKSAGLVVGDNIQKIKGRGKLLMSHMDTVVYLGK--ILAKAPFRVE--GDKA 112
              .: .: * .: *:* .: * .:

ArgE_Ec      YLGTADMKGFFAFIILDALRDVDVTKLKP---LYILATADEETS MAGARYFAETTLRP 162
DapE_Hi     YGRGAADMKGSLAAMIVAAEEYVKANPNHKGTLIALLITSDDEATAKDGTHVVTLMARD 153
ACD_Xc      IGLGVDIKGAAAALVAAANAGDGD-----AAFLFSSDEEANDPR----CIAAFLARG 145
CPG2_Ps     YGPGIADDKGGNAVILHTLKLKEYGVRDYGTITVLENTDEEKGSFG---SRDLIQEEA 168
              * * . * * * * : : .: .: : : * .

ArgE_Ec      D---CAIIGEPTSLQPVRR---AHKHGISNAIRIQGQSGHSS-DPARGVNAIELMHDAI 213
DapE_Hi     EKITYCMVGEPPSAKNLGDVVKNRGRSITGNLYIQGIQGHVA-YPHLAENPIHKAA--- 209
ACD_Xc      LPYDAVLVAEPTMSEAVL-----AHRGISSVLMRFAGRAGHASKQDPAASALHQAMRWG 200
CPG2_Ps     KLADYVLSFEPTSAGDEK---LSLGTSGIAYVQVNTGKASHAGAAPELGVNALVEASDLV 226
              .: ** : . * : : * . * . . . .:

ArgE_Ec      GHILQLRDNLKERYHYEAFVTPYPTLNLGHIHGGDASN-RICACCELHMDIRPLPGMTLN 272
DapE_Hi     ---LFLQELTTYQWDKGNFPPPTSLQIANIHAGTGSNNVIPAELYIQFNLRXYCTEVTDE 266
ACD_Xc      GKALDHVESLAHARFGG---LTGLRFNIGRVDGGIKAN-MIAPAAELRFGRPLPSMDVD 256
CPG2_Ps     LRTMNIDDKAKN-----LRFNWTIAKAGNVSN-IIPASATLNADVRYARNEDFD 274
              .: .: .: .: * * * .: . . * .:

ArgE_Ec      ELNGLLNDALAPVSEWRPGRITVDELHPPIPGYECPNHLQVVEVEKLLGAK---TEVNV 329
DapE_Hi     IIKQKVAEMLEKHNLY--RIEWNLSGKPFLLTKPKLLDSITSAIETIGIT---PKAET 321
ACD_Xc      GLLATFAGFADPAAAHFEETFRGPSLPSGDIAR-AEERRLAARDVADALDLP---IGNAV 312
CPG2_Ps     AAMKTLEERAQQKLEADVVKVIVTRGRPAFNAGEGGKLVDKAVAYYKEAGGTLGVEER 334
              .: .: .: .: .: .: .:

ArgE_Ec      --YCTEAPFIQTLCPVLVLPVGSINQAHQPD--EYLETRFIKPTRELITQVIHHFCWH- 383
DapE_Hi     GGGTSDGRFIALMGAEVVEFGPLNSTIHKVN--ECVSVEDLKGCGEYHKMLVNLDS- 377
ACD_Xc      DFWTEASLFSAGGYTALVYGPVDIAQAHTAD--EFVTLAQLQRYVESVNRILINGSH--- 366
CPG2_Ps     TGGGTDAAYAALSGKPVIESLGLPGFGYHSDKAEYVDISAI PRRLYMAARLIMDLGAGK 393
              .: .: .: .: * : .: .: .:
    
```

Figure 2 Sequence alignment between the structurally characterized enzymes DapE from *H. influenzae*, ACD from *X. campestris*, and CPG₂ from *Pseudomonas sp* strain RS-16 with the ArgE from *E. coli*.

Only the H355A mutant ArgE enzyme was expressed as a soluble enzyme and, consequently, it was the only ArgE mutant investigated *via* kinetic, electronic absorption, and isothermal titration calorimetry (ITC). A three-dimensional homology model of ArgE was also generated using the X-ray crystal structure of the DapE from *Haemophilus influenzae*. Combination of these data provides verification that H355 is an active site ligand and provide new insight into the divalent metal binding properties of co-catalytic metallohydrolase active sites.

Materials and methods

Reagents

All chemicals used were purchased commercially and were of the highest quality available. All metal reagents were obtained from Strem Chemicals, Newburyport, MA with $\geq 99.999\%$ purity. Stock solutions of Co (II) (50 mM) and Zn(II) (10 mM) were prepared by dissolving the metal chloride salts ($\text{CoCl}_2 \cdot 6\text{H}_2\text{O}$ or ZnCl_2) in nanopure water.

Enzyme purification

The aminopeptidase from *Aeromonas proteolytica* (AAP) was purified according to the previously published procedure (Chen et al. 1997). Protein concentrations were estimated from the absorbance at 280 nm using an extinction coefficient $\epsilon_{280} = 41,800 \text{ M}^{-1}\text{cm}^{-1}$ (Bennett and Holz 1997). Wild-type recombinant ArgE from *E. coli* was expressed and purified, as previously described, from a stock culture of *E. coli* BL21 Star™ cells (Invitrogen, Carlsbad, CA) kindly provided by Professor John Blanchard (Javid-Majd and Blanchard 2000). Pure ArgE enzyme (> 98%), as determined by SDS-PAGE gel electrophoresis, was stored at -80°C until used. The concentration of ArgE was estimated from the absorbance at 280 nm using an extinction coefficient $\epsilon_{280} = 41,250 \text{ M}^{-1}\text{cm}^{-1}$ (McGregor et al. 2005). Enzyme concentrations determined by molar absorptivity were in close agreement to that obtained using a Bio-Rad assay.

Site-Directed Mutagenesis

The pET-27a(+) plasmid containing the *argE* gene was extracted and transformed into *E. coli* BL21 Star™ cells for expression of protein variants, which were purified in the same manner as WT ArgE. The Quick Change™ Site-Directed Mutagenesis Kit (Stratagene, La Jolla, CA, USA) and the following primers: 5'-GGC TCA ATT AAT CAG GCT XXX CAA CCT GAT GAA TAT CTG G-3' and 5'-C CAG ATA TTC ATC AGG TTG YYY AGC CTG ATT AAT TGA GCC-3' with GCT and AAA for XXX and AGC and TTT for YYY were employed for production of the H355A and H355K variants respectively. Likewise, 5'-G CTG GCG GGG XXX ACC GAT

ACG GTG CC-3' and 5'-GG CAC CGT ATC GGT YYY CCC CGC CAG C-3' with GCT and AAA for XXX and AGC and TTT for YYY were employed for production of H80A and H80K variants respectively. Products from these Site-Directed Mutagenesis reactions were transformed into *E. coli* XL1-Blue competent cells which were subsequently spread on LB-agar plates containing 100 $\mu\text{g}/\text{mL}$ of Ampicillin. Following over-night incubation at 37°C , one of many colonies from each plate was selected for growth in 50 mL liquid LB medium, containing 100 $\mu\text{g}/\text{mL}$ of Ampicillin, for ≥ 10 hours at 37°C and shaking at 225 rpm. Plasmids were isolated from the resultant cultures using the Qiaprep® Spin Miniprep kit (Qiagen, Valencia, CA) and incorporation of the variant gene sequence was confirmed by DNA sequencing.

Enzymatic assay of ArgE

ArgE activity was measured by the method of Javid-Majd and Blanchard (Javid-Majd and Blanchard 2000). In this assay, the hydrolysis of a 2 mM L-NAO solution, in 50 mM Chelex-100 treated phosphate buffer at pH 7.5, was measured spectrophotometrically at 25°C as the decrease in absorbance at 214 nm ($\Delta\epsilon_{214} = 103 \text{ M}^{-1}\text{cm}^{-1}$), corresponding to the cleavage of the L-NAO amide bond. Protein concentrations were determined using the theoretical value $\epsilon_{280} = 41,250 \text{ M}^{-1}\text{cm}^{-1}$ (Gill and von Hippel 1989). The specific activity of purified wild-type ArgE with L-NAO was typically found to be 2,000 units per mg of enzyme. One unit was defined as the amount of enzyme that releases 1 μmole of ornithine in 60 sec at 25°C . Initial rates were fit directly to the Michaelis-Menten equation to obtain the catalytic constants K_m and k_{cat} .

Preparation of Apo-enzymes

Apo-enzyme samples were prepared for each purified enzyme by methods previously described in the literature (Prescott et al. 1983; Javid-Majd and Blanchard 2000). Briefly, AAP was dialyzed for 72 h at 4°C against 10 mM 1,10-phenanthroline monohydrochloride in 50 mM HEPES buffer, pH 7.5, and then exhaustively dialyzed against Chelex-treated (Chelex-100 column) 50 mM HEPES buffer, pH 7.5. (Bennett and Holz 1997). Apo-ArgE enzyme samples were prepared by adding 15 mM EDTA and incubating for 24 h at 4°C . The EDTA was removed by exhaustive dialysis against Chelex-treated (Chelex-100 column) 50 mM HEPES buffer, pH 7.5, containing 150 mM KCl at 4°C for 36 h. Metal-free buffers were prepared by passing the buffers through a Chelex-100 column. The resulting apo-enzymes were inactive, and were found to contain no detectable metal ions via Inductively Coupled Plasma Atomic Emission Spectrometry (ICP-AES).

Spectroscopic measurements

Electronic absorption spectra were recorded on a Shimadzu UV-3101PC spectrophotometer equipped with a constant temperature holder and a Haake (Type 423) constant temperature-circulating bath. All solutions were degassed prior to performing an experiment. Electronic absorption spectra were normalized for protein concentration and the absorption due to uncomplexed Co(II) ($\epsilon_{512} = 6.0 \text{ M}^{-1} \text{ cm}^{-1}$) (D'souza et al. 2000).

Isothermal Titration Calorimetry

Isothermal Titration Calorimetry (ITC) measurements were carried out on a MicroCal OMEGA ultrasensitive titration calorimeter at $25 \pm 0.2^\circ\text{C}$. The divalent metal ion titrants and apo-enzyme solutions were prepared in 25 mM Chelex-100 treated HEPES buffer at pH 7.5. Stock buffer solutions were thoroughly degassed before each titration. The enzyme solution ($70 \mu\text{M}$) was placed in the calorimeter cell and stirred at 200 rpm to ensure rapid mixing. Typically, 4–6 μL of titrant was delivered over 7.6 s with 6 min. intervals between injections to allow for complete equilibration. Each titration was continued until 4.5–6 equiv. of M(II) had been added to ensure that no additional complexes were formed in excess titrant. A background titration, consisting of the identical titrant solution but only the buffer solution in the sample cell, was subtracted from each experimental titration to account for heat of dilution. Individual AAP solutions were prepared by diluting stock enzyme solutions with 50 mM Chelexed HEPES buffer (pH 7.5), and ArgE solutions were prepared by diluting stock enzyme solutions with 25 mM Chelexed HEPES buffer (pH 7.6) containing 150 mM KCl.

Molecular modeling

A three-dimensional homological structure of the ArgE from *E. coli* was developed using the X-ray crystal structure of the DapE from *H. influenzae* (PDB code:3IC1) as a template (Figure 3) (Rowse et al. 1997; Eswar et al. 2003; Krissinel and Henrick 2004; Nocek et al. 2010). Sequence analysis of the target and template show that these two proteins are of similar length, share good sequence identity (~24%), and exhibit no significant sequence gaps. The ModWeb-based homology-building server was used to construct a structural homology model of the ArgE from *E. coli*. Comparison of the energy minimized ArgE homology model to the X-ray crystal structure of DapE, using the MathMaker in UCSF Chimera, reveals that the ArgE homology model displays the typical dimerization and catalytic domains of DapE with a Needleman-Wunsch (Needleman and Wunsch 1970) score of 490.6 and an average RMSD of 0.974 \AA for the core atom pairs (Figure 3).

Results and discussion

Protein production

Of the four ArgE mutant plasmids produced (H355A, H355K, H80A and H80K) and transformed into *E. coli* BL21 Star™ cells, only ArgE H355A was produced as a soluble enzyme. SDS-PAGE analyses of protein from *E. coli* cultures hosting plasmids containing the other three ArgE variants indicated that the enzymes were produced in abundance, but in an insoluble form. Various attempts were made to refold inclusion bodies of the three insoluble ArgE variants, but none proved fruitful.

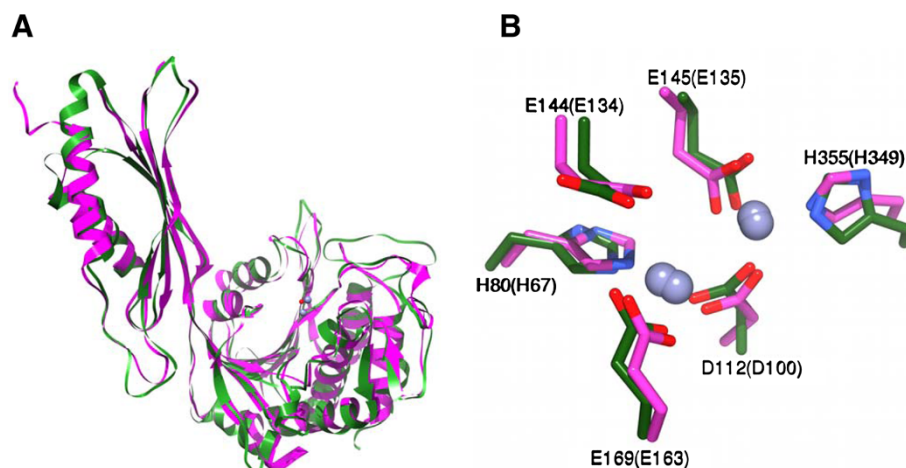


Figure 3 Homology model of the [ZnZn(ArgE)] from *E. coli* based on the X-ray structure of DapE. A) Overlay of the ArgE homology model (Green) and the X-ray crystal structure of DapE (Magenta). The two Zn(II) ions and the bridging water from ArgE are shown as spheres. **B)** Conserved active site residues for ArgE (Green) and DapE (Magenta). Nitrogen atoms are in blue, oxygen atoms are in red. The residues are labeled with single-letter amino acid codes with the labels for residues from DapE in parenthesis.

Kinetic studies on ArgE H355A

Based on ICP-AES data, the as-purified H355A ArgE mutant enzyme contains no Zn(II) ions. These data imply that the remaining metal binding site in ArgE has a much higher K_d value and is unable to bind Zn(II) in the absence of saturating conditions, similar to DapE, and consistent with weak cooperative binding as suggested by EXAFS (Tao et al. 2012; Gillner et al. 2009). The hydrolysis of L-NAO by H355A was monitored in the presence of three equivalents of Zn(II) or Co(II), after a one-hour incubation period, at pH 7.5 (Figure 1). Interestingly, no enzymatic activity was detected for H355A ArgE in the presence of three equivalents of Zn(II). The lack of measurable activity for the H355A mutant enzyme may be the result of the reaction conditions used. Since the amide bond cleavage of L-NAO is monitored at 214 nm, enzyme concentrations must be < 10 nM so as not to overwhelm the amide bond absorption of L-NAO with background protein absorption. The severely reduced/eliminated enzymatic activity is consistent with the impaired ability of this variant to bind Zn(II). This further substantiates the hypothesis that this point mutation has knocked out a key metal ligand.

Further verification of this hypothesis comes from examining the hydrolysis of L-NAO by the Co(II)-loaded H355A variant. The WT Co(II)-loaded ArgE enzyme is 2.4-times more active than the WT Zn(II)-loaded form. For Co(II)-loaded H355A ArgE, a k_{cat} value of 10 ± 1 s⁻¹ was obtained in the presence of three equivalents of Co(II) using L-NAO as the substrate ($K_m = 0.5 \pm 0.1$ mM). Comparison of the kinetic parameters for

the Co(II)-loaded WT and H355A ArgE enzymes indicate that the decrease in activity of H355A is due to a ~ 380 -fold decrease in k_{cat} . Interestingly, the K_m value determined for the Co(II)-loaded H355A mutant enzyme is smaller than Co(II)-loaded WT ArgE by ~ 2 -fold. Calculation of the catalytic efficiency (k_{cat}/K_m) for the Co(II)-loaded H355A mutant enzyme results in a value ~ 160 -fold less than the Co(II)-loaded WT ArgE. The histidine to alanine mutation at this position, while having some impact on substrate binding, has primarily affected a key aspect of the active site of the enzyme (*i.e.* metal cofactor binding).

Electronic absorption spectra of Co(II)-loaded ArgE

Insight into whether H355 acts as an active site Zn(II) ligand was also investigated by examining the electronic absorption spectra of the Co(II)-substituted forms of the enzyme (Figure 4). The addition of one equivalent of Co(II) to apo-H355A ArgE (in Chelex-100 treated 50 mM HEPES buffer at pH 7.5) results in a broad absorption band with maxima at 560 nm ($\epsilon_{560} = \sim 95$ M⁻¹ cm⁻¹) along with shoulders at 515 nm ($\epsilon_{515} = \sim 75$ M⁻¹ cm⁻¹) and 620 nm ($\epsilon_{620} = \sim 55$ M⁻¹ cm⁻¹) suggesting that the Co(II) ion bound to H355A ArgE resides in a penta-coordinate geometry (Bertini and Luchinat 1984; Horrocks et al. 1980). The addition of a second equivalent of Co(II) to H355A ArgE did not alter the overall shape of the observed absorption spectrum but did approximately double the molar absorptivity, consistent with a coordination number of five. In contrast, the WT ArgE from *E. coli* in the presence of one equivalent of Co(II) exhibited three distinct peaks at 560, 619, and 705 nm

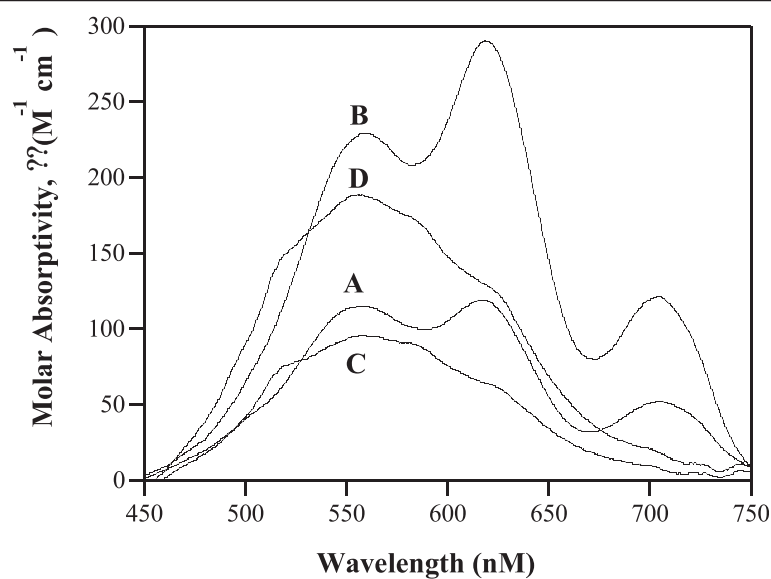


Figure 4 UV-vis absorption spectra of 1 mM samples of (A) WT ArgE in the presence of 1 equivalent of Co(II), (B) WT ArgE in the presence of 2 equivalents of Co(II), (C) H355A ArgE in the presence of 1 equivalent of Co(II), and (D) H355A ArgE in the presence of 2 equivalents of Co(II). (Reaction conditions: 25°C in 50 mM HEPES buffer, pH 7.5, and 150 mM KCl).

with ϵ values of $\epsilon_{560} = 114 \text{ M}^{-1}\text{cm}^{-1}$, $\epsilon_{619} = 119 \text{ M}^{-1}\text{cm}^{-1}$, and $\epsilon_{705} = 52 \text{ M}^{-1}\text{cm}^{-1}$, respectively (McGregor et al. 2005). The addition of a second equivalent of Co(II) increased the intensity of each of the observed absorption bands, providing ϵ values of $\epsilon_{560} = 229 \text{ M}^{-1}\text{cm}^{-1}$, $\epsilon_{619} = 290 \text{ M}^{-1}\text{cm}^{-1}$, and $\epsilon_{705} = 121 \text{ M}^{-1}\text{cm}^{-1}$, respectively (Figure 4). Thus, the UV-vis spectrum of H355A ArgE is significantly different from WT ArgE in the presence of one and two equivalents of Co(II) (Figure 4) and the loss of distinct d-d transitions in the UV-vis spectrum of H355A is likely the result of a more flexible distorted five-coordinate geometry with water molecules occupying non-protein coordination sites. Taken together, these data are consistent with the loss of an active site histidine ligand.

The altered ability of the H355A ArgE to bind Co(II) was also investigated by titrating Co(II) into apo-H355A ArgE samples and monitoring the molar absorptivity of the λ_{max} for the Co(II) *d-d* bands, which allowed the dissociation constant (K_d) for this divalent metal binding site to be obtained by fitting these titration data to equation 1 (Winzor and Sawyer 1995):

$$r = pC_s / (K_d + C_s) \quad (1)$$

where p is the number of sites for which interaction with Co(II) is governed by the intrinsic dissociation constant K_d , C_s is the free metal concentration and, r is the binding function calculated by conversion of the fractional saturation (f_a) (Winzor and Sawyer 1995). Values for K_d and p were obtained by fitting these data *via* an iterative process that allowed K_d and p to vary (Figure 5). The

best fits obtained for Co(II) binding to the H355A ArgE provided a p value of 0.9 and a K_d value of $1.6 \pm 0.3 \mu\text{M}$, which is 4-fold larger than that observed for WT ArgE ($K_d = 0.4 \mu\text{M}$) (McGregor et al. 2005) consistent with a loss of an active site ligand. Since alteration of H355 will greatly perturb and potentially alter the ability of metal binding, this K_d value likely corresponds to a single metal binding event. Moreover, the K_d value obtained for Co(II) binding to H355A is ~ 4 times stronger than that obtained for Zn(II) binding to WT ArgE. This difference is typically related to Zn(II)'s preference for four or five-coordinate geometries *vs.* Co(II)'s preference for five or six-coordinate structures (Holz 2002). These data, taken together with the lack of observed activity for H355A ArgE in the presence of Zn(II), suggest that H355 is in fact an active site ligand.

Isothermal Titration Calorimetry

Additional insight into whether H355 is a ligand in the active site of ArgE and which metal binding site it resides in, were gleaned by obtaining K_d values and thermodynamic profiles using ITC (Figure 6). These data were analyzed with a one, two, or three-site binding model after subtraction of the background heat of dilution, *via* an interactive process using the Windows-based Origin software package supplied by MicroCal. This software package uses a nonlinear least-squares algorithm, which allows the concentrations of the titrant and the sample to be fit to the heat-flow-per-injection to an equilibrium binding equation. The K_d value, enzyme-metal stoichiometry (n), and the change in enthalpy (ΔH°) were allowed to vary during the fitting process.

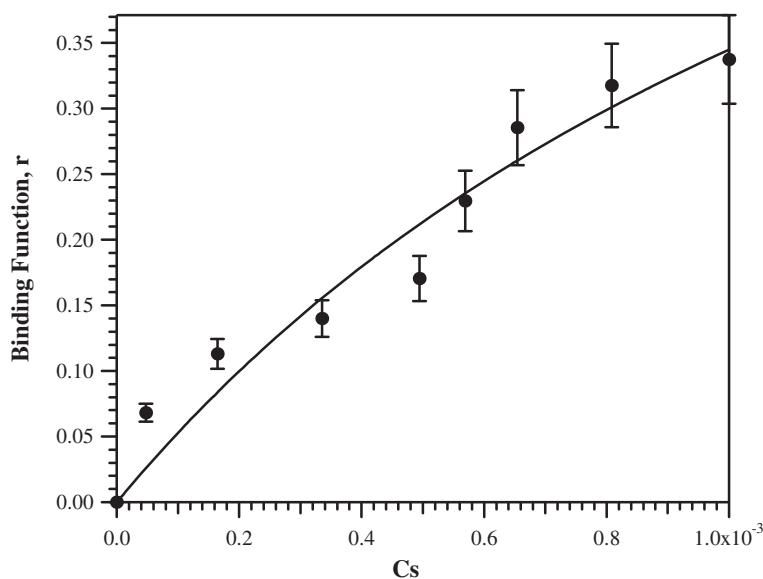


Figure 5 Plot of $\Delta\epsilon_{560}$ vs. the concentration of free Co(II) ions in solution for Co(II) titration into apo-H355A ArgE (50 mM KH_2PO_4 buffer, pH 7.5).

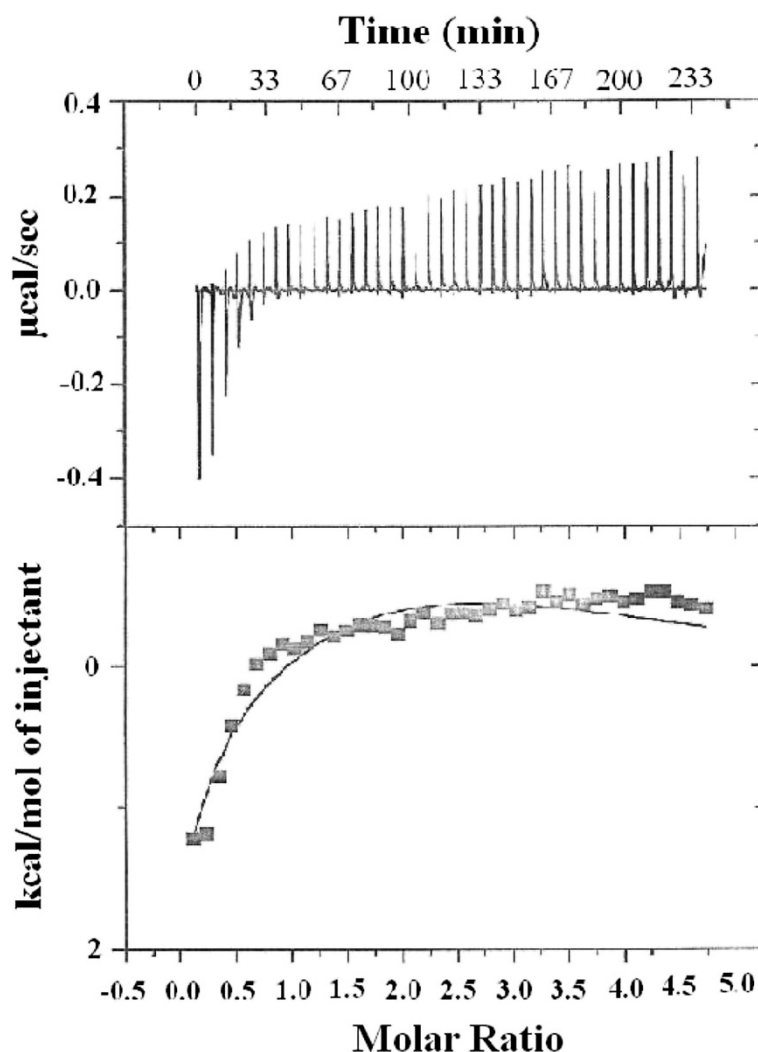


Figure 6 (Top) ITC titration data for a 70 μM solution of apo- H355A ArgE with a 2.5 mM solution of Zn(II). (Bottom) Fit of the ITC data for H355A ArgE after subtracting the heat of dilution. (Reaction conditions: 25°C in 50 mM HEPES buffer, pH 7.5, and 150 mM KCl).

The equilibrium binding constant, K_a , and the enthalpy change ΔH , were used to calculate ΔG and ΔS using the Gibbs free energy relationship (equation 2):

$$\Delta G^\circ = -RT \ln[K_a] = \Delta H^\circ - T\Delta S^\circ \quad (2)$$

where $R = 1.9872 \text{ cal mol}^{-1} \text{ K}^{-1}$. The relationship between K_a and K_d is defined as:

$$K_d = 1/K_a \quad (3)$$

For the H355A ArgE mutant, the best fits provided n values of 2 for two non-interacting sites with K_d values of 39 and 330 μM (Figure 6; Table 1). The ITC data do not suggest cooperative binding whereas the EXAFS data do; however, weak cooperative binding is typically undetectable *via* ITC. The ΔH° value for the first Zn (II) binding event is endothermic with a large positive

entropy consistent with the loss of water ligands from the Zn(II)-hexaaquo complex upon Zn(II) binding to ArgE. On the other hand, the second Zn(II) binding event is exothermic with an entropy change near zero (Table 2).

Table 1 Metal dissociation constants of ArgE H355A and WT ArgE determined by ITC and UV-vis absorption titration

Enzyme	Metal	Method	K_{d1} (μM)	K_{d2} (μM)
WT ArgE ^a	Zn(II)	ITC	2.7	51
H355A ArgE	Zn(II)	ITC	39	330
WT ArgE ^a	Co(II)	ITC	0.4	153
H355A ArgE	Co(II)	UV-vis Titration	1.6	ND ^b

^aPreviously reported (ref. (McGregor et al. 2005)).

^bNone detected.

Table 2 Thermodynamic binding parameters for Zn(II) binding to AAP, WT ArgE and H355A ArgE (ΔH (kcal/mol), (ΔG cal/mol·K) and (ΔS cal/mol·K))

Parameter	AAP	WT ArgE ^a	H355A ArgE
ΔH_1	2.1	4.6	6.0
ΔH_2	1.1	-2.7	-3.7
ΔG_1	-11.0	-5.9	-6.0
ΔG_2	-7.5	-7.6	-4.7
ΔS_1	43	35	40
ΔS_2	29	16	3.5

^aPreviously reported (ref. (McGregor et al. 2005)).

Comparison of these data with previously reported ITC data for Zn(II) binding to WT ArgE and DapE provide insight into which metal binding site is being populated first in the H355A ArgE mutant enzyme (McGregor et al. 2005; Davis et al. 2006). Both ArgE and DapE bind two Zn(II) ions in non-interactive

binding sites with K_d values for the first Zn(II) binding event for ArgE and DapE being 2.7 and 4.4 μM , respectively, whereas the observed K_d values for the second metal binding event in ArgE and DapE are 51 and 13.6 μM , respectively. The ΔH° values observed for the first Zn(II) binding event in both ArgE and DapE are endothermic while the second is exothermic (Table 2). While K_d for AAP has been reported previously by one of us (Bzymek et al. 2005), we report here a high quality ITC data set for Zn(II) binding to AAP, which provided K_d values for the first and second metal binding event of 0.008 and 0.4 μM , respectively (Figure 7). The energy change observed for both AAP binding sites indicates an endothermic-type reaction with the second metal binding event providing a more negative ΔH° value than the first. Taken together, the thermodynamic data obtained for H335A are similar to those observed for the first binding events in WT ArgE, DapE, and AAP, suggesting that the H335 residue resides in the second

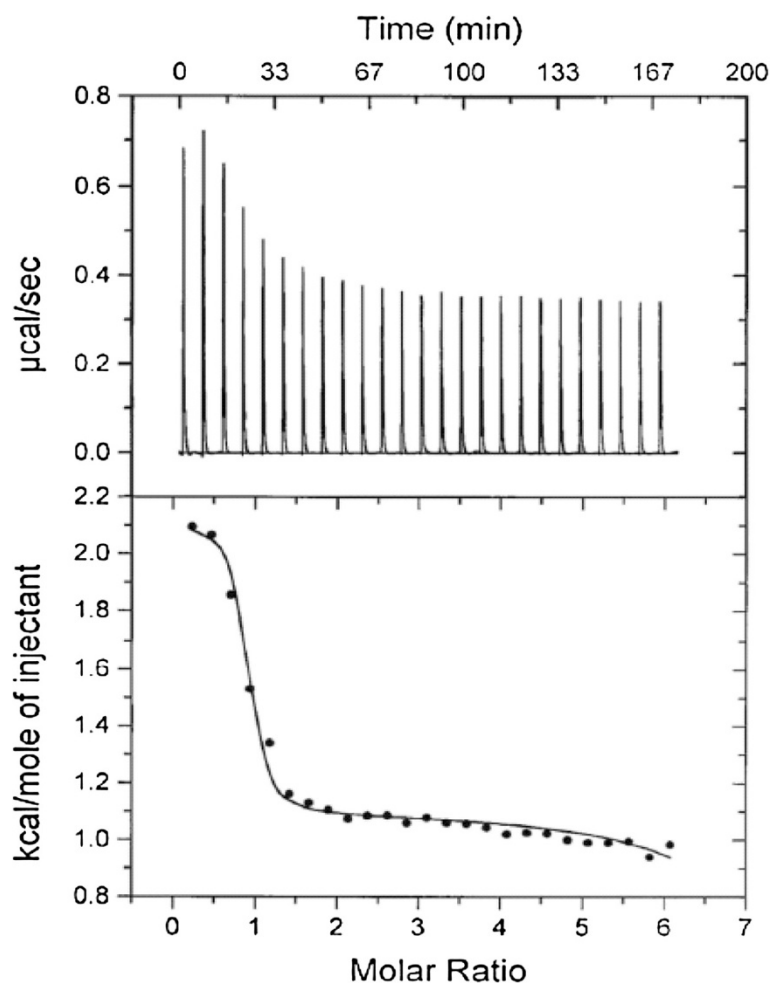


Figure 7 (Top) ITC titration data for 30 μM solution of AAP with a 2.5 mM Zn(II) solution. **(Bottom)** Fit of the ITC data for AAP after subtraction of the heat of dilution. (Reaction conditions: 25°C in 50 mM HEPES buffer, pH 7.5).

metal binding site similar to that observed for DapE (Gillner et al. 2009; Nocek et al. 2010). The weaker binding affinity for the first Zn(II) binding event in H355A ArgE vs. WT ArgE is likely the result of weak cooperative binding, which would be lost upon mutation of H355.

Modeling of the ArgE structure

Since no three-dimensional X-ray crystal structure has been reported for the ArgE from *E. coli*, a three-dimensional homological structure was developed using the X-ray crystal structure of the DapE from *H. influenzae* (PDB code:3IC1) as a template (Figure 3) (Rowell et al. 1997; Eswar et al. 2003; Krissinel and Henrick 2004; Nocek et al. 2010). The catalytic domain of ArgE contains the dinuclear Zn(II) site with a Zn-Zn distance of ~ 3.3 Å and within 4.0 Å of the Zn(II) binding sites of ArgE, and all of the amino acid residues are nearly identical to those observed in DapE confirming the assignment of H80 and H355 as active site ligands in ArgE (Figure 3) (Rowell et al. 1997; Eswar et al.

2003; Krissinel and Henrick 2004). The active site in ArgE is located in a long and open cleft of the catalytic domain; the cleft is parallel to and in the vicinity of the “hinge” region between the catalytic domain and the dimerization domain (Figure 8). With such a location, conformational changes upon metal and/or substrate binding are likely and have been observed for DapE (Nocek et al. 2010). Both Zn(II) ions are solvent accessible and have four protein centered ligands including H80 and H355 as well as two terminal glutamate residues (E145 and E160) and a bridging aspartate residue (D122). A bridging water provides the fifth ligand for both metal ions, which forms a hydrogen bond to a second water molecule that is in turn hydrogen bonded to E144, a candidate for the general acid/base during catalysis (Davis et al. 2006). Therefore, our data supports the hypothesis that H355 is an active site Zn(II) ligand, and as this residue corresponds to H349 in DapE, which has been shown to be the second metal binding site, it is likely that H355 resides in the second metal binding site of ArgE.

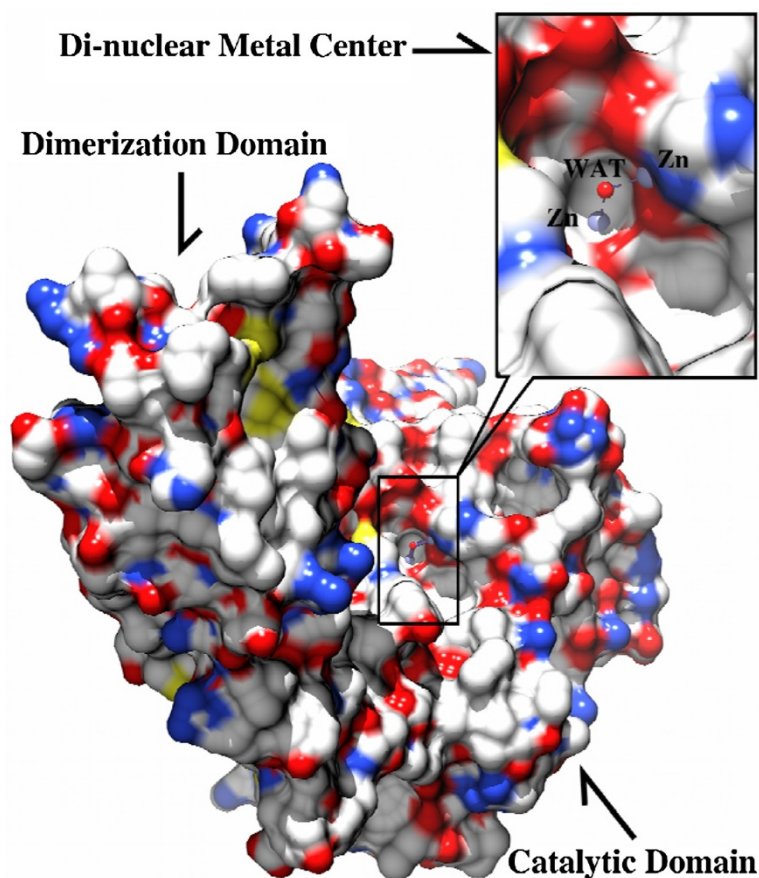


Figure 8 Surface rendering of the [ZnZn(ArgE)] molecule where the black box indicates the position of the di-nuclear metal center. Insert: Close-up of the dinuclear Zn(II) cluster showing that the active site is located in a long cleft across the catalytic domain. Zn(II) ions are shown in light blue spheres and the bridging water molecule is shown as a red sphere and labeled as “WAT”.

Summary

The kinetic, spectroscopic and thermodynamic data presented herein provide evidence that H355 is intimately involved in catalysis and serves as a metal binding ligand. While these data do not conclusively indicate which metal binding site H355 resides in, they are consistent with H355 residing in the second metal binding site, similar to DapE. Therefore, the ArgE from *E. coli* forms a (μ -aquo)(μ -carboxylato)dizinc(II) core where H80 and H355 function as active site metal ion ligands similar to DapE, AAP, and CPG₂ and consistent with EXAFS data (Tao et al. 2012). While the data reported here provide a structural starting point for elucidating the catalytic mechanism of ArgE, which may lead to the design and synthesis of small molecule inhibitors that specifically target ArgE, an X-ray crystal structure of the ArgE from *E. coli* with both one and two metal ions bound is desperately needed.

Abbreviations

ArgE: *argE*-encoded *N*-acetyl-L-ornithine deacetylase; DapE: *dapE*-encoded *N*-succinyl-L,L-diaminopimelic acid desuccinylase; AAP: aminopeptidase from *Vibrio proteolyticus* (*Aeromonas proteolytica*); ACD: *N*-acetyl-L-citrulline deacetylase from *Xanthomonas campestris*; CPG₂: carboxypeptidase from *Pseudomonas sp.* strain-RS-16; L-NAO: *N*⁶-acetyl-L-ornithine; EDTA: Ethylenediaminetetraacetic acid; HEPES: 4-(2-hydroxyethyl)-1-piperazineethanesulfonic acid; Tris: tris(hydroxymethyl)aminomethane; Tricine: *N*-tris(hydroxymethyl)methylglycine; SDS-PAGE: Sodium Dodecyl Sulfate-Polyacrylamide Gel Electrophoresis; ITC: Isothermal Titration Calorimetry; ICP-AES: Inductively Coupled Plasma Atomic Emission Spectrometry.

Competing interests

The authors declare that they have no competing interests.

Authors' contribution

WM be carried out the molecular biology studies and sequence alignments. DG purified AAP and conducted spectroscopic studies. SS did all ITC studies. DL prepare the homology model. RH is the principal investigator and drafted the manuscript. All authors read and approved the final manuscript.

Acknowledgements

This work was supported by the National Institutes of Health (R15 AI085559-01A1, RCH).

Author details

¹Contribution from the Department of Chemistry, Marquette University, Milwaukee, WI 53233, USA. ²Chemistry and Biochemistry, Loyola University Chicago, Chicago, IL 60626, USA. ³The Department of Chemistry, Silesian University of Technology, Gliwice 44-100, Poland. ⁴The Department of Applied Sciences and Mathematics, College of Technology and Innovation, Arizona State University, Mesa, AZ 85212, USA.

Received: 30 April 2013 Accepted: 28 August 2013

Published: 23 September 2013

References

Bennett B, Holz RC (1997) EPR studies on the mono- and dicobalt(II)-substituted forms of the aminopeptidase from *Aeromonas proteolytica*. Insight into the catalytic mechanism of dinuclear hydrolases. *J Am Chem Soc* 119:1923–1933

Bertini I, Luchinat C (1984) High-spin cobalt(II) as a probe for the investigation of metalloproteins. *Adv Inorg Biochem* 6:71–111

Born TL, Zheng R, Blanchard JS (1998) Hydrolysis of *N*-succinyl-L,L-Diaminopimelic Acid by the *Haemophilus influenzae* *dapE*-Encoded Desuccinylase: Metal Activation, Solvent Isotope Effects, and Kinetic Mechanism. *Biochemistry* 37:10478–10487

Bzymek KP, Moulin A, Swierczek SI, Ringe D, Petsko GA, Bennett B, Holz RC (2005) Kinetic, Spectroscopic, and X-ray Crystallographic Characterization of the Functional E151H Aminopeptidase from *Aeromonas proteolytica*. *Biochemistry* 44(36):12030–12040, 10.1021/bi0505823

Chen G, Edwards T, D'souza VM, Holz RC (1997) Mechanistic studies on the aminopeptidase from *Aeromonas proteolytica*: A two-metal ion mechanism for peptide hydrolysis. *Biochemistry* 36:4278–4286

Chevrier B, Schalk C, D'Orchymont H, Rondeau J-M, Moras D, Tarnus C (1994) Crystal Structure of *Aeromonas proteolytica* Aminopeptidase: A Prototypical Member of the Co-Catalytic Zinc Enzyme Family. *Structure* 2(4):283–291

Cunin R, Glandsdorff N, Pierard A, Stalon V (1986) Biosynthesis and metabolism of arginine in bacteria. *Microbiol Rev* 50:314–352

D'souza VM, Bennett B, Copik AJ, Holz RC (2000) Characterization of the Divalent Metal Binding Properties of the Methionyl Aminopeptidase from *Escherichia coli*. *Biochemistry* 39:3817–3826

Davis RH (1986) Compartmental and regulatory mechanisms in the arginine pathways of *Neurospora crassa* and *Saccharomyces cerevisiae*. *Microbiol Rev* 50:280–313

Davis R, Bienvenue D, Swierczek SI, Gilner DM, Rajagopal L, Bennett B, Holz RC (2006) Kinetic and Spectroscopic Characterization of the E134A- and E134D- Altered *dapE*-Encoded *N*-Succinyl-L, L-Diaminopimelic Acid Desuccinylase from *Haemophilus influenzae*. *J Biol Inorg Chem* 11:206–216

Desmarais W, Bienvenue DL, Bzymek KP, Petsko GA, Ringe D, Holz RC (2006) The High-Resolution Structures of the Neutral and the Low pH Crystals of the Aminopeptidase from *Aeromonas proteolytica*. *J Biol Inorg Chem* 11:398–408

Eswar N, John B, Mirkovic N, Fiser A, Ilyin VA, Pieper U, Stuart AC, Marti-Renom MA, Madhusudhan MS, Yerkovich B, Sali A (2003) Tools for comparative protein structure modeling and analysis. *Nucleic Acids Res* 31:3375–3380

Gill SC, Von-Hippel PH (1989) Calculation of protein extinction coefficients from amino acid sequence data. *Anal Biochem* 182:319–326

Gillner DM, Bienvenue DL, Nocek BP, Joachimiak A, Zachary V, Bennett B, Holz RC (2009) The *dapE*-Encoded *N*-Succinyl-L, L-Diaminopimelic Acid Desuccinylase from *Haemophilus influenzae* Contains Two Active Site Histidine Residues. *J Biol Inorg Chem* 14:1–10

Grodeau J-M, Agouridas C, Masson MRP, LeGoffic F (1986) The Lysine Pathway as a Target for a New Genera of Synthetic Antibacterial Antibiotics? *J Med Chem* 29:1023–1030

Hani EK, Ng D, Chan VL (1999) Arginine biosynthesis in *Campylobacter jejuni* TGH9011: determination of the argCOBD cluster. *Can J Microbiol* 45:959–969

Holz RC (2002) The Aminopeptidase from *Aeromonas proteolytica*: Structure and Mechanism of Co-Catalytic Metal Centers Involved in Peptide Hydrolysis. *Coord Chem Rev* 232:5–26

Holz RC, Bzymek K, Swierczek SI (2003) Co-Catalytic Metallopeptidases as Pharmaceutical Targets. *Cur Opin Chem Biol* 7:197–206

Horrocks W, DeW I Jr, Holmquist B, Thompson JS (1980) Structural and electronic mimics of the active site of cobalt(II)-substituted zinc metalloenzymes. *J Inorg Chem* 12:131–141

Javid-Majd F, Blanchard JS (2000) Mechanistic analysis of the *argE*-encoded *N*-acetylornithine deacetylase. *Biochemistry* 39:1285–1293

Krissinel E, Henrick K (2004) Secondary-structure matching (SSM), a new tool for fast protein structure alignment in three dimensions. *Acta Crystallogr D: Biol Crystallogr* 60:2256–2268

Ledwidge R, Blanchard JS (1999) The dual biosynthetic capability of *N*-acetylornithine aminotransferase in arginine and lysine biosynthesis. *Biochemistry* 38:3019–3024

McGregor W, Swierczek SI, Bennett B, Holz RC (2005) The *argE*-Encoded *N*-Acetyl-L-Ornithine Deacetylase from *Escherichia coli* Contains a Dinuclear Metallo-Active Site. *J Am Chem Soc* 127:14100–14107

Meinert T, Schmitt E, Mechulam Y, Blanquet S (1992) Structural and biochemical characterization of the *Escherichia coli* *argE* gene product. *J Bacteriol* 174:2323–2331

Needleman B, Wunsch CD (1970) A General Method Applicable to the Search for Similarities in the Amino Acid Sequence of Two Proteins. *J Mol Biol* 48(443–453):443–453

Nocek BP, Gillner DM, Fan Y, Holz RC, Joachimiak A (2010) Structural Basis for Catalysis by the Mono- and Dimetalated Forms of the *dapE*-Encoded *N*-succinyl-L, L-Diaminopimelic Acid Desuccinylase. *J Mol Biol* 397(3):617–626, 10.1016/j.jmb.2010.01.062

Picard FJ, Dillon JR (1989) Cloning and organization of seven arginine biosynthesis genes from *Neisseria gonorrhoeae*. *J Bacteriol* 171:1644–1651

Prescott JM, Wagner FW, Holmquist B, Vallee BL (1983) One hundred fold increased activity of *aeromonas* aminopeptidase by sequential substitutions

- with Ni(II) or Cu(II) followed by zinc. *Biochem Biophys Res Commun* 114:646–652
- Rowse S, Paupit RA, Tucker AD, Melton RG, Blow DM, Brick P (1997) Crystal Structure of Carboxypeptidase G2, a Bacterial Enzyme with Applications in Cancer Therapy. *Structure* 5:337–347
- Sakanian VA, Ovespian AS, Mett IL, Kochikian AV, Petrosian PK (1990) Molecular cloning and structural-functional analysis of the arginine biosynthesis genes of the thermophilic bacterium *Bacillus stearothermophilus*. *Genetika* 26:1915–1925
- Sakanyan V, Petrosyan P, Lecocq M, Boyen A, Legrain C, Demarez M, Hallet JN, Glansdorff N (1996) Genes and enzymes of the acetyl cycle of arginine biosynthesis in *Corynebacterium glutamicum*: enzyme evolution in the early steps of the arginine pathway. *Microbiol* 142:99–108
- Shi D, Yu X, Roth L, Tuchman M, Allewell NM (2007) Structure of a novel N-acetyl-L-citrulline deacetylase from *Xanthomonas campestris*. *Biophys Chem* 126:86–93
- Tao Y, Shokes JE, McGregor WC, Scott RA, Holz RC (2012) Structural characterization of Zn(II)-, Co(II)-, and Mn(II)-loaded forms of the argE-encoded N-acetyl-L-ornithine deacetylase from *Escherichia coli*. *J Inorg Biochem* 111:157–163, 10.1016/j.jinorgbio.2012.02.005
- Valentsev VE, Krupenina VI, Mishan'kin BN (1995) The deamination of L-arginine and the synthesis of active nitrogen compounds in *Yersinia pestis*. *Zh Mikrobiol Epidemiol Immunobiol* 5:48–51
- Velasco AM, Leguina JI, Lazcano A (2002) Molecular evolution of the lysine biosynthetic pathways. *J Mol Evol* 55:445–459
- Winzor DJ, Sawyer WH (1995) Quantitative Characterization of Ligand Binding. Wiley-Liss, New York
- Xu Y, Liang Z, Legrain C, Rüger HJ, Glansdorff N (2000) Evolution of arginine biosynthesis in the bacterial domain: novel gene-enzyme relationships from psychrophilic Moritella strain (*Vibrionaceae*) and evolutionary significance of N-alpha-acetyl ornithinase. *J Bacteriol* 182:1609–1615

doi:10.1186/2193-1801-2-482

Cite this article as: McGregor et al.: Identification of a Histidine Metal Ligand in the argE-Encoded N-Acetyl-L-Ornithine Deacetylase from *Escherichia coli*. *SpringerPlus* 2013 **2**:482.

Submit your manuscript to a SpringerOpen[®] journal and benefit from:

- Convenient online submission
- Rigorous peer review
- Immediate publication on acceptance
- Open access: articles freely available online
- High visibility within the field
- Retaining the copyright to your article

Submit your next manuscript at ► springeropen.com
